Received: 16 February 2023 | Revised: 2 August 2023 | Accepted: 20 August 2023

DOI: 10.1002/mp.16709

RESEARCH ARTICLE

MEDICAL PHYSICS

Robust mixed electron-photon radiation therapy planning for soft tissue sarcoma

Veng Jean Heng[1] | **Monica Serban**[2,3] | **Marc-André Renaud**[4] | **Carolyn Freeman**[5] | **Jan Seuntjens**[2,3,6]

[1]Department of Physics and Medical Physics Unit, McGill University, Montreal, Canada

[2]Princess Margaret Cancer Centre and Department of Radiation Oncology, University of Toronto, Toronto, Canada

[3]Gerald Bronfman Department of Oncology, Medical Physics Unit, McGill University, Montreal, Canada

[4]Gray Oncology Solutions, Montreal, Canada

[5]McGill University Health Centre, Montreal, Canada

[6]Department of Medical Biophysics, University of Toronto, Toronto, Canada

Correspondence
Veng Jean Heng, Department of Physics and Medical Physics Unit, McGill University, 1001 Boulevard Décarie Rm. DS1.5029, Montréal, QC, H4A 3J1, Canada.
Email: veng.heng@mail.mcgill.ca

Funding information
Fonds de recherche du Québec – Nature et technologies, Grant/Award Number: 290039; Canadian Institutes of Health Research, Grant/Award Number: FDN-143257

Abstract

Background: Mixed electron-photon beam radiation therapy (MBRT) is an emerging technique in which external electron and photon beams are simultaneously optimized into a single treatment plan. MBRT exploits the steep dose falloff and high surface dose of electrons while maintaining target conformity by leveraging the sharp penumbra of photons.

Purpose: This study investigates the dosimetric benefits of MBRT for soft tissue sarcoma (STS) patients.

Material and methods: A retrospective cohort of 22 STS of the lower extremity treated with conventional photon-based Volumetric Modulated Arc Therapy (VMAT) were replanned with MBRT. Both VMAT and MBRT treatments were planned on the Varian TrueBeam linac using the Millenium multi-leaf collimator. No electron applicator, cutout or additional collimating devices were used for electron beams of MBRT plans. MBRT plans were optimized to use a combination of 6 MV photons and five electron energies (6, 9, 12, 16, 20 MeV) by a robust column generation algorithm. Electron beams in this study were planned at standard 100 cm source-axis distance (SAD). The dose to the clinical target volume (CTV), bone, normal tissue strip and other organs-at-risk (OARs) were compared using a Wilcoxon signed-rank test.

Results: As part of the original VMAT treatment, tissue-equivalent bolus was required in 10 of the 22 patients. MBRT plans did not require bolus by virtue of the higher electron entrance dose. CTV coverage by the prescription dose was found to be clinically equivalent between plans of either modality: V_{50Gy}(MBRT) $= 97.9 \pm 0.2\%$ versus V_{50Gy}(VMAT) $= 98.1 \pm 0.6\%$ (p=0.34). Evaluating the absolute paired difference between doses to OARs in MBRT and VMAT plans, we observed lower V_{20Gy} to normal tissue in MBRT plans by $14.9 \pm 3.2\%$ ($p < 10^{-6}$). Similarly, V_{50Gy} to bone was found to be decreased by $8.2 \pm 4.0\%$ ($p < 10^{-3}$) of the bone volume.

Conclusion: For STS with subcutaneous involvement, MBRT offers statistically significant sparing of OARs without sacrificing target coverage when compared to VMAT. MBRT plans are deliverable on conventional linacs without the use of electron applicators, shortened source-to-surface distance (SSD) or bolus. This study shows that MBRT is a logistically feasible technique with clear dosimetric benefits.

KEYWORDS
mixed beam radiation therapy, planning study, soft tissue sarcoma

1 | INTRODUCTION

Soft tissue sarcoma (STS) is a rare malignant tumor with 13 190 new cases estimated in the United States in 2022.[1] Although STS can affect any site of the body, the majority arise in the extremities with 59% of them localized.[2] Treatment consists of surgical resection with negative margins. Many will also receive preoperative radiation therapy to reduce the risk of local recurrence after surgery alone.[3] Image-guided radiation therapy has allowed for more conformal treatment, leading to lower doses to normal tissues and lower risk of wound complications.[4,5] The use of bolus (tissue-equivalent material placed on patient's skin) may be needed for cases where the clinical target volume (CTV) involves skin or subcutaneous tissue that would not receive an adequate dose otherwise.[3] The use of bolus is however associated with greater risk of skin toxicity[6] and the variability in its preparation results in greater uncertainty in planning dose calculations. The American Society for Radiation Oncology (ASTRO) guidelines recommend against the routine use of tissue-equivalent bolus for most sarcomas.[3]

The feasibility and potential benefits of modulated electron radiation therapy (MERT), delivered using either additional collimators[7–14] or the photon multi-leaf collimators (pMLC),[7,15–18] is addressed in a number of studies. By leveraging the limited penetration depth and high surface dose of electron beams, electron-only MERT treatment plans were shown to deliver lower doses to normal tissue than photon-only plans. This however comes at the cost of worse target dose homogeneity.[18,19] Mixed electron-photon beam radiation therapy (MBRT) delivered using an existing pMLC is an emerging technique in which both external electron and photon beam are simultaneously optimized into a single treatment plan.[20–26] MBRT has been shown to provide superior sparing of normal tissue without sacrificing target coverage.[20,22–24] For tumors with superficial involvement, MBRT offers the possibility of excellent target coverage without the use of bolus. The steep depth dose curve of electron beams allow MBRT plans to better spare healthy tissue and organs-at-risk (OAR) at depths beyond the tumor. Electron apertures in MBRT deliveries are collimated using only the existing pMLC. Due to significant electron scatter in air, the penumbra of electron beams collimated with pMLC is known to be wider at larger source-to-surface distance (SSD).[15,27] Deliveries of electron apertures in MERT and MBRT plans have therefore so far been thought to require shortened SSD of 70–80 cm.[28]

Patient setup error is traditionally accounted for in photon-based radiotherapy by using the concept of a planning target volume (PTV).[29] Assuming an adequate choice of margins, by prescribing the dose to the PTV, the CTV will receive the prescription dose despite setup errors or patient/organ motion. The underlying assumption in this method is that the static dose cloud approximation holds: the spatial dose distribution is not significantly affected by changes in patient positioning. This assumption has been shown to not hold true in the case of charged particles and has lead to the development of robust optimization for intensity modulated proton therapy.[30] Using a similar approach, Renaud et al. implemented robust optimization in the context of MBRT.[25] They showed that MBRT plans must be robustly optimized to properly account for patient setup and motion uncertainties. In this particular implementation, dose distributions are calculated explicitly in additional error scenarios where a positioning error is artificially introduced. The cost function can then be calculated as a weighted average of the cost function of each scenario. Accurate deliveries of robust MBRT plans have been experimentally validated on conventional linacs with excellent agreements between Monte Carlo-calculated doses and ion chamber and film measurements.[26,31]

This study seeks to demonstrate the applicability and benefits of MBRT for STS of the extremity. By performing a retrospective treatment planning study, MBRT is dosimetrically compared to the standard of care: photon-based Volumetric Modulated Arc Therapy (VMAT).

2 | METHODS

2.1 | Patient selection

A retrospective cohort of 22 STS patients was selected among 38 consecutive patients treated at the McGill University Health Centre between December 2017 and June 2021. All patients completed a 25-fraction photon-only VMAT preoperative treatment on a Varian TrueBeam linear accelerator (Varian Medical Systems, Palo Alto, CA). Only patients with STS of the lower extremity, without tumor extent above the groin or within the foot or ankle, were chosen. This was done to keep the patient geometry within the cohort to be mostly homogeneous. Exclusion criteria included interrupted treatments, CTVs length >36 cm in the cranial-caudal direction, CTV size >14 cm in the axial plane, or CTV location being unsuitable for electron treatments. Unsuitable CTV location refers to CTVs starting either too deep (>1 cm from the skin) or whose shallow regions are obstructed by OARs such as the contralateral leg. The exclusion of patients with too long or large CTV is such that the memory size of beamlets do not exceed our cluster's maximum memory during MBRT plan optimization. The consort diagram in Figure 1 enumerates the number of patients excluded for each criterion. The median tumor size, as measured by its largest

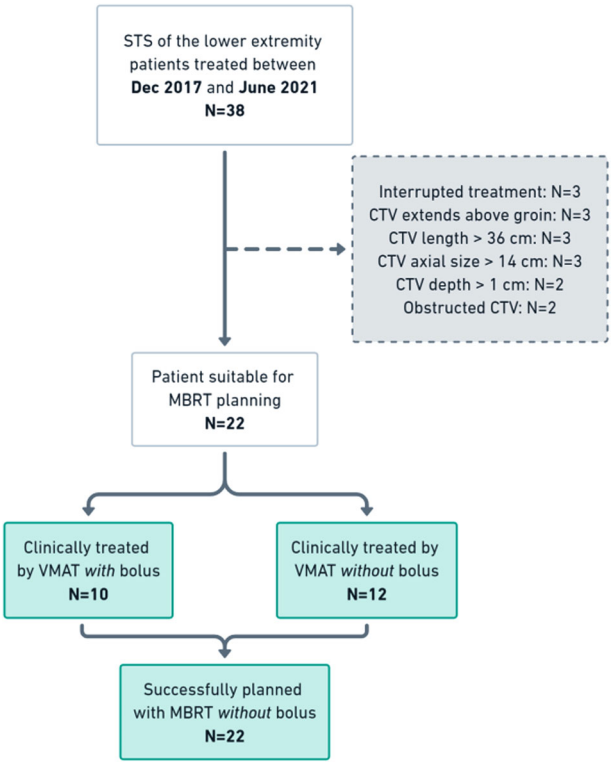

FIGURE 1 Consort diagram describing patient selection criteria. A total of 38 patients with STS of the lower extremity (excluding foot and ankle) were treated between Dec. 2017 and June 2021. Twenty-two patients were eligible for the planning study. Bolus was not used for any patients for MBRT plans. The CTV length, size and depths are illustrated in Figure 2. CTV, clinical target volume; MBRT, Mixed electron-photon beam radiation therapy; STS, soft tissue sarcoma.

diameter, was 11.7 cm. For comparison, the median tumor size of the Radiation Therapy Oncology Group (RTOG) 0630 trial's cohort B was 10.5 cm.[5] Written institutional permission for the use of anonymized patient treatment planning data was obtained from the Quality Improvement Committee of the Department of Radiation Oncology at the McGill University Health Centre. The relevant recommendations given in the RATING guidelines[32] were followed in this study.

2.2 | Clinical treatment planning and dose prescription

Planning was performed on a computed tomography (CT) scan of the patient in the treatment position with 3 mm slice thickness and pixel spacing of around 1 mm. All CT scans were obtained on the Philips Brilliance Big Bore scanner (Philips, Amsterdam, Netherlands) in one of the following patient position: feet first supine (n=19), feet first prone (n=1), or head first supine (n=2). Patients were immobilized with a Vac-Lok device. Magnetic Resonance Imaging studies were co-registered with CT images to aid the contouring of the gross tumor volume (GTV). For GTVs larger than 8 cm, the CTV was contoured with 1.5 cm axial margins and 3 cm cranial-caudal margins from the GTV. For smaller tumors, CTV axial margins of 1 cm and cranial-caudal margins of 2 cm were used as per RTOG 0630 and our standard practice. CTV contours did not include any intact bony structures. When skin surfaces were not involved by gross tumor, CTVs were cropped 3–5 mm from the skin (n=12). If the gross tumor involved the skin and bolus was used, CTVs were not cropped (n=10). While following the same skin cropping rule as the CTV, the PTV consisted of a 5 mm geometrical expansion from the CTV.

TABLE 1 Dose constraints to OAR used for evaluation of both clinical and MBRT plans.

OAR	Dose constraint
Bone	$D_{mean} < 37$ Gy
	$V_{50Gy} < 50\%$
Femoral head	$D_{mean} < 40$ Gy
Joint	$V_{50Gy} < 50\%$
Normal tissue strip	$V_{20Gy} < 50\%$
Skin	$D_{max} < 51.5$ Gy
Anus	$V_{30Gy} < 50\%$
Genitalia	$V_{30Gy} < 50\%$
Testes	$V_{3Gy} < 50\%$

Abbreviations: OAR, organs-at-risk; MBRT, Mixed electron-photon beam radiation therapy.

Contoured OARs relevant for plan optimization included the following: normal tissue strip, skin, bone, joints, testes, genitalia, anus. The dose constraints to the OARs used for evaluation of treatment plans are tabulated in Table 1. These constraints aim to reduce long-term sequelae such as edema, fibrosis, joint stiffness and bone fracture. For consistency, the normal tissue strip OAR was uniformly contoured as the subtraction of the PTV + 5 mm margin and any bone from the leg contour, on axial slices within 2 cm proximal and distal to the PTV. An example of this contour is shown in Figure 2. The ipsilateral bone contour is limited to PTV axial slices, so as to only include bone within the radiation field as described in the RTOG 0630 protocol.[5]

VMAT treatment planning of clinical plans were performed on the Eclipse (versions 11 and 15) treatment planning system (TPS). For VMAT plans, a dose of 50 Gy (2 Gy/fraction) was prescribed to 95% of the PTV. Although planning strategy varied according to the planner, highest priority was given to lower and upper optimization constraints on target structures. Optimization constraints and priority for each OAR were chosen according to their volume, their distance from the target, and their position with respect to the beam arrangement. The maximum dose to the PTV was generally restrained

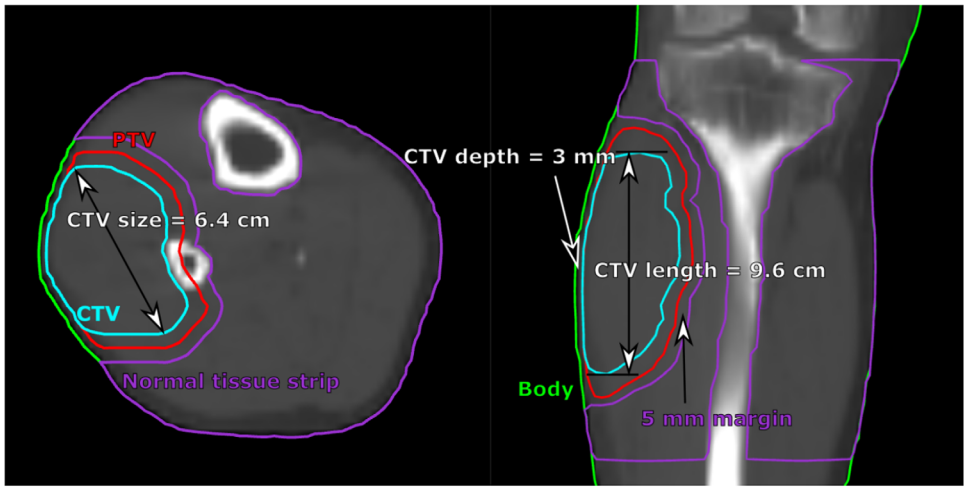

FIGURE 2 Axial (left) and coronal (right) CT slices of a representative patient. The CTV size, depth and length used as exclusion criteria in Figure 1 are illustrated with arrows. The normal tissue strip is uniformly contoured as the rest of the limb excluding any bone and a 5 mm margin around the PTV. CT, computed tomography; CTV, clinical target volume; PTV, planning target volume.

to below 107% of the prescription dose. Doses to OARs were minimized while ensuring that the constraints in Table 1 are met. In exceptional cases, OAR constraints were exceeded to meet PTV coverage. For plan optimization purposes, patient doses were calculated with the Analytical Anisotropic Algorithm (AAA). At the time of planning, the dose distribution was calculated on a 2.5×2.5×3.0 mm^3 grid. The VMAT plans consisted of either 2 or 3 arcs of 6 MV flattened photon beams delivered at different collimator angles. Control points were set at gantry angle intervals of 2°. Only the Varian Millennium multi-leaf collimator (MLC) was used.

2.3 | MBRT planning

All patient plans and CT images were exported from Eclipse and imported to our in-house TPS "*Brems*". "*Brems*" is a TPS hosted as a web app that was developed as a rewrite of the old "*Radify*" TPS[22,33] to better accommodate MBRT treatment planning. It integrates the necessary components of the MBRT treatment planning workflow in one platform: selection of gantry angles, beamlet calculation, beamlet-based optimization, dose recalculation with Monte Carlo, evaluation of plan quality using Dose-Volume Histogram (DVH) and other dose statistics, generation of plan files in `.dcm` or `.xml` formats, and so forth.

MBRT treatments were planned on the same TrueBeam linac originally used for VMAT treatment. For each patient, 3–4 and 5–8 beam angles were selected for the electron and photon components, respectively. Both electron and photon beams were planned as step-and-shoot apertures at standard source-axis distance (SAD) of 100 cm. Both photons and electrons were collimated with the Millennium photon-MLCs. As such, electron fields were planned without the use of standard electron applicators and cutouts.

For each beam angle, the beam's eye view plane is divided into a regular square grid. The dose distribution due to radiation traversing one grid element is referred to as a beamlet. Beamlets were calculated at five electron energies (6, 9, 12, 16, and 20 MeV) and at a 6 MV photon beam with flattening filter. A pre-calculated Monte Carlo method was used to efficiently calculate electron beamlets using pre-calculated electron tracks.[34,35] Photon beamlets were calculated using an in-house collapsed cone convolution superposition algorithm.[22] The particle source for both these methods were generated from Varian-provided phase space files. Electron phase space files had their energy tuned to match measured data.[31] All beamlet calculations were performed on graphics processing units. Beamlets were robustly calculated to account for positioning uncertainty. This was done by calculating each beamlet in six equally weighted additional scenarios, in addition to the nominal (non-shifted) scenario. In each shifted scenario, the isocenter is translated by 5 mm in one of the following directions: cranial-caudal, anterior-posterior and lateral right-left.

A robust column generation optimizer[25] was used to perform simultaneous photon and electron beamlet optimization of MBRT plans. Optimization constraints were applied on the following structures (if applicable): CTV, contralateral leg, ipsilateral bone, testes, and 2 mm skin strip. A normal tissue objective (NTO) function was employed to enforce a rapid dose fall-off in voxels outside the CTV. The NTO penalizes voxels exceeding a pre-assigned threshold dose. The threshold dose is calculated based on the voxel's distance to the CTV. The plan was normalized such that the average $\bar{V}_{50Gy}$ over all seven scenarios of CTV volumes receiving 50 Gy

is 95%. It must be noted that for MBRT plans, robust optimization is performed on the CTV rather than the traditional PTV-based optimization.

In this study, no MBRT plans made use of bolus. For the purpose of MBRT planning, any bolus present in the CT (n=10) had its density overridden to air. For these 10 patients, the CTV in the MBRT plan was cropped 2 mm from the skin to allow for buildup in the absence of bolus. This cropped CTV was used for the evaluation of both the VMAT and MBRT plan. As such, any dose comparison presented in this study is performed on identical structures.

The planning aim for MBRT consisted of ensuring similar or better dose homogeneity in the CTV as its VMAT counterpart while minimizing dose to bone and the normal tissue strip. In practice, this was achieved by starting with strict NTO parameters to demand sharp dose fall-offs and progressively relaxing them at following optimization iterations until the CTV dose homogeneity was satisfactory. To be deemed acceptable, the near-maximum dose D2% to the CTV in MBRT plans had to remain strictly below 110%. Doses to OAR had to meet the constraints of Table 1, except in cases where the VMAT plan was also unable to meet the constraint. In general, planning objective weights for each structure were set in the following descending priority order: CTV, skin, NTO, testes, bone, contralateral leg. The active planning time spent per patient by the planner and the total time (including time waiting for dose calculation and optimization) was recorded. As this is a retrospective study, the VMAT planning times could not be obtained for comparison.

For plan evaluation, patient doses were recalculated in all seven robust scenarios with an EGSnrc[36] Monte Carlo model using Varian TrueBeam phase space files. All voxels within the patient body contour were set to water with variable density assigned via a CT-to-mass density curve, exported from Eclipse. As such, dose-to-water is reported in this study. Dose calculations were performed on uniform voxels of dimension 2.5 $\times$ 2.5 $\times$ 2.5 mm^3. For a fair comparison, the dose of the clinical VMAT plan was also robustly recalculated using the same Monte Carlo model. The same positioning shifts were introduced in the robust calculation of either treatment modalities. No renormalization or re-optimization of the VMAT plan was performed at this step.

To distinguish the dosimetric impact of a mixed modality treatment from the robust optimization process, an additional non-robust MBRT plan was generated for one representative patient. For this plan, target coverage constraints and prescription were applied on the PTV, as is done in the VMAT plan. All other constraints were otherwise kept identical to the robust MBRT plan. This was only done for illustrative purpose, as a realistic implementation of MBRT should always be done robustly.

2.4 | Plan evaluation and statistical analysis

The DVH of all patients was computed for the CTV, the ipsilateral bone and the normal tissue strip for each treatment modality. The DVH of the nominal scenario of all 22 plans were aggregated and the mean of each DVH point and its standard error were calculated. The cohort's mean DVH is calculated by evaluating the mean volume receiving at least x Gy over all 22 plans at every dose point x ranging from 0 to the maximum dose received by the structure in any plan.

For each OAR, the dose metrics tabulated in Table 1 were evaluated for both modalities and compared to their corresponding constraints. In particular, the dose to skin in VMAT plans were found to be distinctly different between patients that required bolus usage and those that did not. As such, for the purpose of the comparison of skin dose, patients were also separated according to their use or non-use of bolus during their VMAT treatment.

The dose conformity to the CTV was evaluated using the following definition of the conformity index:

$$CI = \frac{\text{isodose volume}}{\text{clinical target volume}}, \quad (1)$$

where the isodose volume corresponds to the sum of volume within the body contour that exceeds a given isodose level. A conformity index of one would thus correspond to the case where the isodose volume equates the CTV. This conformity index was calculated for multiple isodose levels (40%, 60%, 80% and 95%) to compare the dose fall-off rate of either modality. The near-maximum dose D2% to the CTV was also evaluated in both plans. For both treatment modalities, all DVHs and dose metrics were evaluated on *Brems* using the same methodology. Differences in any metrics between MBRT and VMAT plans were evaluated with a two-tailed Wilcoxon signed-rank test using the *SciPy* library on Python. Statistical significance is assumed for $p < 0.05$. Differences between all uncertainties on mean or median values in this study are reported with a coverage factor of $k = 2$.

To give a depiction of the composition of an MBRT plan, the mean CTV dose due to the photon component and each electron energy was evaluated. The overall distribution was represented in a boxplot to show the variance of electron versus photon usage across the cohort.

3 | RESULTS

All 22 patients were successfully planned with MBRT with clinically acceptable plan quality. The mean DVH over the distribution of all 22 patients is plotted in

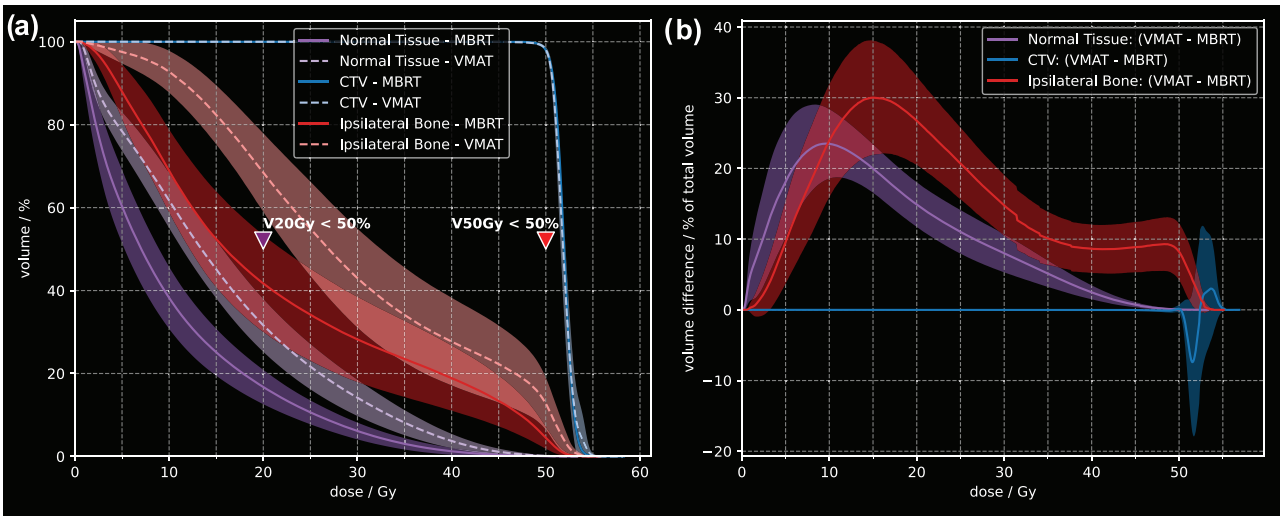

FIGURE 3 (a) Average DVH of all 22 patients. Lines represent the mean DVH for each structure and the bands represent the 2 σ confidence interval on the mean. The planning constraints for the two OARs are plotted as inverted triangles. MBRT plans show equivalent CTV DVH to VMAT with significant reduction in dose to normal tissue and bone. (b) Average difference DVH of all 22 patients. Lines represent the mean difference in DVH between the VMAT and the MBRT plan for each patient, while the bands represent the two σ confidence interval on the mean difference. CTV, clinical target volume; DVH, Dose-Volume Histogram; MBRT, Mixed electron-photon beam radiation therapy; OARs, organs-at-risk; VMAT, Volumetric Modulated Arc Therapy.

Figure 3a for both the MBRT and VMAT plans. The DVH bands represent the $\pm 2\sigma$ standard error on the mean. MBRT plans provide equivalent CTV DVH as compared to VMAT. In the nominal scenario, the CTV's coverage by the prescription dose was found to be equivalent in either modality: V_{50Gy}(MBRT) $= 97.9 \pm 0.2\%$ versus V_{50Gy}(VMAT) $= 98.1 \pm 0.6\%$ ($p = 0.34$, Wilcoxon signed-ranked test). The dose to normal tissue and bone, which are the two common OARs in all sarcoma patients, was found to be significantly lower in MBRT plans. For each patient, the DVH of the MBRT plan was subtracted from that of the VMAT plan to show the decrease in dose to OARs in Figure 3b. For normal tissue, V_{20Gy} was reduced on average by $14.9 \pm 3.2\%$ in MBRT plans ($p < 10^{-6}$). For bone, V_{50Gy} decreased on average by $8.2 \pm 4.0\%$ of the bone volume ($p < 10^{-3}$). The dose constraints for the remaining OARs are evaluated for each plan and plotted in Figure 4a as a scatter plot. V_{50Gy} to the joint and D_{mean} to the femoral head and to the bone were found to be significantly lower in MBRT plans according to a two-tailed Wilcoxon signed-ranked test (mean reduction of 4.0 ± 2.9 % $p = 0.003$, 4.7 ± 4.4 Gy $p = 0.03$, and 8.0 ± 1.4 Gy $p < 10^{-6}$, respectively). No significant difference was found in the evaluated metric of the other OARs of Figure 4a. For VMAT plans, the dose metrics are evaluated on the Monte Carlo-recalculated dose and can significantly differ from the AAA dose used during treatment planning. This lead to one plan being shown to violate testes constraints despite originally meeting them at the time of planning.

The near-maximum dose $D_{0.5cc}$ to a 2 mm thick contour of the skin is plotted in Figure 4b. Patients were separated according to their bolus usage in the clinical VMAT plan, while no MBRT plans used bolus. MBRT plans had significantly lower ($p = 0.002$) median $D_{0.5cc}$ (50.7 ± 0.5 Gy) than VMAT plans (52.5 ± 0.4 Gy) in patients that had used bolus. However, in patients that did not use bolus, $D_{0.5cc}$ was found to be significantly higher ($p < 10^{-3}$) in MBRT plans (48.5 ± 0.5 Gy) than in VMAT plans (42.8 ± 2.6 Gy) due to the higher electron surface dose.

The conformity index to the CTV was evaluated for four isodose levels to compare the rate of the dose fall-off and plotted in Figure 4c. At 95% of the prescription dose, both the MBRT and VMAT plans for all patients have a CI larger than one. At the 40% isodose level (20 Gy), the median CI was found to be significantly smaller in MBRT plans: 2.4 ± 0.3 versus 3.3 ± 0.3 for VMAT ($p < 10^{-6}$). This indicates a more rapid dose fall-off in MBRT plans outside the CTV, such that a smaller volume of the body is subjected to lower dose baths.

The near-maximum dose D2% to the CTV is also plotted in Figure 4d. MBRT plans were found to have a statistically significantly higher D2% than VMAT plans: median $D2\%_{MBRT} = 53.6 \pm 0.2$ Gy versus $D2\%_{VMAT} = 53.2 \pm 0.2$ Gy, $p = 0.046$. This difference can also be observed in the slightly wider CTV DVH curve in MBRT plans in Figure 3a. Nevertheless, as the difference in D2% is small in magnitude, the CTV homogeneity would be deemed practically equivalent in clinical practice.

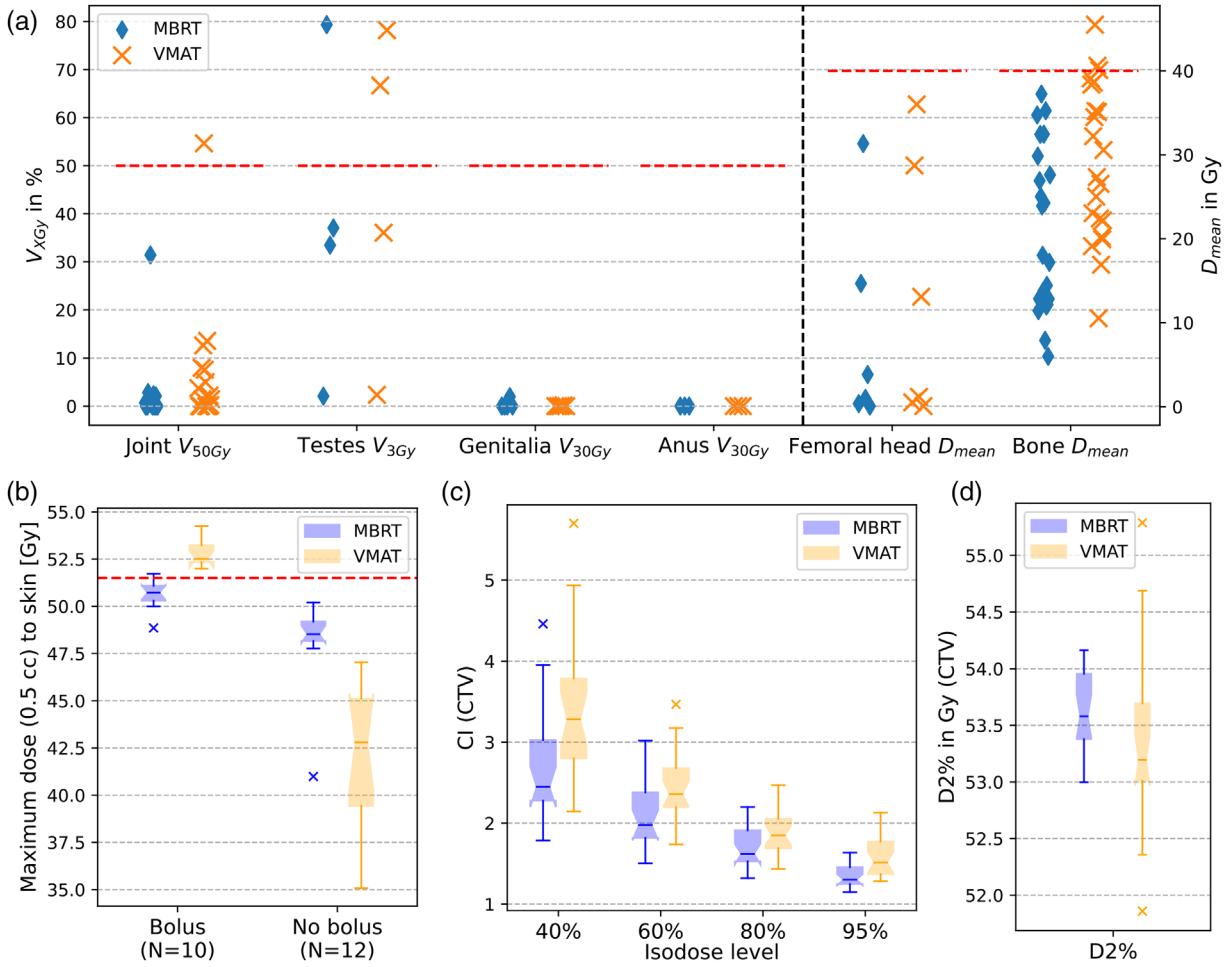

FIGURE 4 (a) Comparison of the dose to various OARs. The metric evaluated for each OAR are obtained from Table 1. The red dotted lines represent the maximum constraint for each metric. Doses to the joint, the femoral head and to the whole ipsilateral bone were found to be significantly lower in MBRT plans according to a Wilcoxon signed-ranked test. (b) Near-maximum (0.5 cc) dose to 2 mm skin. The maximum dose constraint to skin (51.5 Gy, 103% of the prescription dose) is drawn with red dotted lines. Patients are separated according to their bolus usage in their VMAT plans. No bolus was used in any of the MBRT plans. (c) Conformity index to the CTV for different isodose levels. (d) Near-maximum dose D2% to the CTV. Lines within the boxplots represent the median of each distribution. Notches represent the 95% confidence interval on the median. Outliers, calculated to be lying beyond 1.5× the interquartile range, are illustrated as crosses. CTV, clinical target volume; MBRT, Mixed electron-photon beam radiation therapy; OAR, organs-at-risk; VMAT, Volumetric Modulated Arc Therapy.

A comparison of the two modalities is depicted in Figure 5 for a representative patient of the cohort. Bolus was used for the VMAT treatment of this patient but was overridden to be air for MBRT planning. For the four isodose levels that were evaluated (20%, 40%, 80% and 100% of the prescription dose), the isodose volumes were consistently smaller in the MBRT plan (Figure 5a). This illustrates the steeper dose fall-off that is characteristic to MBRT. Due to this effect, a lower dose to both the normal tissue strip and bone can be observed over almost the entirety of their DVH curves in Figure 5b. The shaded DVH bands represent the robust range of DVH values as evaluated over seven positioning scenarios. Without resorting to bolus, the CTV DVH of the MBRT plan can be seen to overlap with the VMAT's DVH, indicating equivalent target coverage. The 50 Gy isodose shows higher dose conformity and bone sparing of the MBRT plan, while CTV is adequately covered in all robust scenarios as evidenced by the overlapping CTV bands.

To evaluate the contribution of photons and each electron energy in MBRT plans, the mean CTV dose due to each component is plotted as a boxplot in Figure 6. Although there is considerable variation across plans, the CTV dose is overall somewhat evenly distributed between electrons versus photons. Among electron energies, the higher energies have a significantly larger contribution to the mean CTV dose. Nevertheless, it must be noted that lower electron energies tend to be responsible for doses in specific spatial regions of the target (e.g., more superficial regions). Therefore, when averaged over the entire CTV, their mean CTV dose will

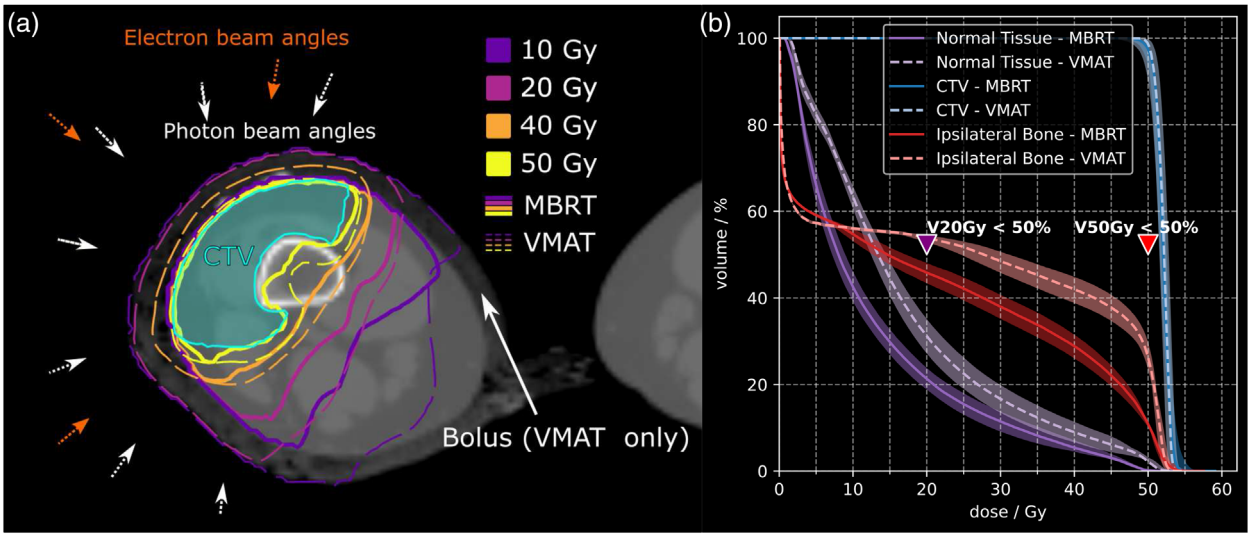

FIGURE 5 (a) Comparison of four isodose levels between MBRT (full lines) and VMAT (dashed lines) plans for a representative patient. The MBRT plan can be observed to have a more rapid dose fall-off outside the CTV. The angles of electron (orange) and photon (white) beams in the MBRT plan are illustrated as arrows. The bolus visible in the CT image is only taken into account in the calculation of the VMAT plan; it is overridden to be air for MBRT calculations. The CTV being shown was cropped 2 mm from the skin to allow for buildup in the bolus-free MBRT plan. (b) Comparison of the DVH of the MBRT (full lines) and VMAT (dashed lines) plans for the same patient. The shaded bands represent the range of DVH values attained over seven positioning scenarios. The CTV evaluated in both the MBRT and VMAT DVHs corresponds to the aforementioned cropped CTV. CT, computed tomography; CTV, clinical target volume; DVH, Dose-Volume Histogram; MBRT, Mixed electron-photon beam radiation therapy; OAR, organs-at-risk; VMAT, Volumetric Modulated Arc Therapy.

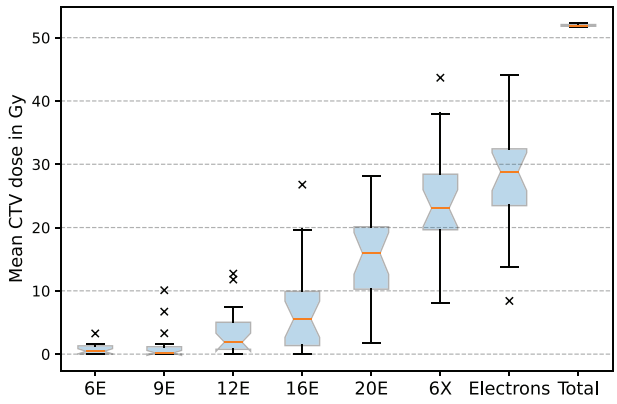

FIGURE 6 Distribution of the dose contribution towards the mean CTV dose due to each energy component of MBRT plans. The sum of electrons contribution and the total contribution of all components are also plotted for reference. Higher electron energies and photons have a higher contribution to the mean CTV dose. CTV, clinical target volume; MBRT, Mixed electron-photon beam radiation therapy.

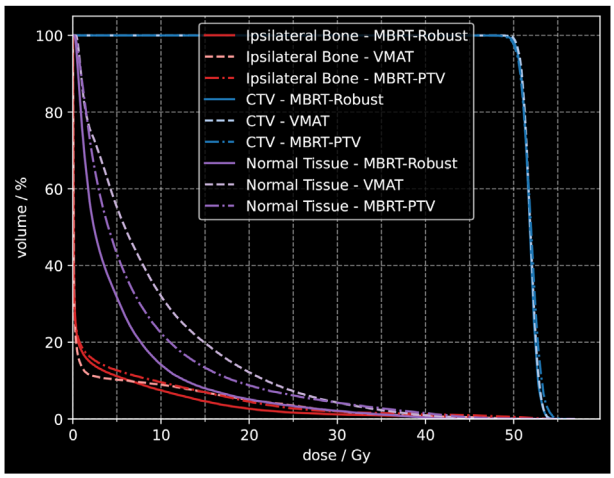

FIGURE 7 DVH of one representative patient featuring three plans: the robustly optimized MBRT plan, the clinical VMAT plan and a PTV-optimized MBRT plan. Both the robustly optimized and PTV-optimized MBRT plans used the same optimization constraints. The PTV-optimized MBRT plan shows superior sparing of normal tissue compared to VMAT due to the sharper electron dose fall-off with depth. However, even more sparing is achieved in the robustly-optimized MBRT plan. DVH, Dose-Volume Histogram; MBRT, Mixed electron-photon beam radiation therapy; PTV, planning target volume; VMAT, Volumetric Modulated Arc Therapy.

appear smaller due to the smaller volume in which they have a dose contribution.

For one representative patient, an additional non-robust PTV-based MBRT plan was generated and compared to the robust MBRT and non-robust VMAT plans in Figure 7. The CTV's V_{50Gy} was evaluated to be similar in the three plans: 97.4%, 98.2% and 99.2% in the PTV-based MBRT, robust MBRT and VMAT plans, respectively. On the other hand, both MBRT plans offered better sparing of the normal tissue strip than VMAT with V_{20Gy}(MBRT-PTV) = 8.8% and V_{20Gy}(MBRT-Robust) = 5.1% vs. V_{20Gy}(VMAT) = 12.2%.

On average, MBRT plans required around 1 h of active planning time, with less than three optimization attempts for most cases. However, the total planning time took on

average 3 days due to the time-consuming robust beamlet calculations, robust optimization, and robust Monte Carlo recalculation.

A RATING score of 98% was achieved and the score sheet is provided in the *Supplementary material*.

4 | DISCUSSION

In STS, higher nominal doses have been associated with increased edema and bone fracture rate.[6,37] Lower incidence of late toxicities in two phase II clinical trials[4,5] is attributed to smaller target volumes. To reduce the risk of long-term sequelae, doses outside the target should therefore be minimized. The average DVH difference plot in Figure 3b shows consistently lower dose volumes at practically all dose points to the normal tissue contour and bone in the MBRT plan. The normal tissue was systematically contoured to be the subtraction of the PTV + 5 mm margin and bone contours from the limb contour. Therefore, this result indicates that on average, MBRT plans deliver significantly less dose outside the target. This effect is even more pronounced when examining volumes subjected to low dose baths. As the dose of electron beams falls off much more rapidly with depth than photon beams, MBRT subjects fewer voxels beyond the target to low dose baths.

The dose to the CTV was found to feature slightly higher hot spots in MBRT plans as indicated by the D2% in Figure 4d. As MLC-collimated electron beams at SSD 100 cm have inherently wider penumbras than photon beams and a distinct depth dose curve, their usage tends to increase the dose heterogeneity within the CTV. MBRT as a technique aims to compensate for this downside by using both electrons and photons. More electron usage tends to decrease doses beyond the target at the cost of target homogeneity. This is an optimization problem that is defined by the constraints and weights chosen by the planner. MBRT plans were observed to have a median D2% to the CTV of 53.6 ± 0.2 Gy ($\approx$107% of the prescription dose), 0.4 Gy higher than their VMAT counterpart. As per the RTOG 0630 protocol, no more than 20% of the PTV must receive more than 110% of the prescription dose (= 55 Gy in this study). This criterion was met by all MBRT and VMAT plans in this study.

In routine clinical practice, for photon planning without bolus, the PTV needs to be cropped 5 mm from the surface to leave enough tissue for buildup to occur. If a higher superficial dose is required, a tissue equivalent bolus is used to raise the dose to the surface. In theory, despite the superficial target, the skin should still be spared from excessive dose as it is associated with a higher risk of wound healing complications. However, controlling the dose downstream from the bolus is difficult when the prescription dose must be met in the target and the reproducibility of bolus setup is uncertain. This leads to high doses to skin as observed in Figure 4b which exceed the maximum skin dose constraint of 103% of the prescription dose. With MBRT, a thinner buildup region is required due to the electron's higher entrance dose. As such, it provides the option of sparing 2 mm of skin while also adequately covering the rest of the target without using bolus. For this reason, for plans that used bolus with VMAT (n=10), we have opted to crop the CTV 2 mm from the surface. In fact, the dose to the 2 mm of skin is further restricted in MBRT plans such that its near-maximum dose meet the 103% constraint (Figure 4b). At the time of surgery, if there is suspicion of skin involvement, any underdosed skin would also be resected. It is important to note that for these 10 plans, the cropped CTV has been used for dose evaluation of both VMAT and MBRT. Therefore, for every patient in this study, any dose metrics that is compared between VMAT versus MBRT is reported on identical CTVs.

Of the 22 patients that were planned in this study, 10 patients required the use of bolus for their original VMAT treatment. In contrast, no patients required the use of bolus in MBRT plans. Similarly, Mueller et al. have shown for a superficial chest wall case that the plan quality of MBRT plans was not significantly affected by the absence of bolus.[23] Bolus usage entails significant logistical effort in the clinical workflow. Bolus must be positioned in similar conditions during simulation and at every fraction of the treatment. It is difficult to quantify the difference in bolus thickness and density at each instance. This introduces a substantial uncertainty on the dose to the skin and to the target in the VMAT delivery. Bolus usage has been associated with increased frequency of chronic skin telangiectasias.[6] Although the use of bolus has not been directly correlated with major wound complications,[38,39] it tends to increase the dose to skin as can be seen in Figure 4b. Higher doses to skin can lead to acute skin toxicity such as radiation dermatitis.[40] Moreover, LeBrun et al. found radiation dermatitis to be a predictor of wound complications in STS.[39]

When bolus was not used with VMAT (n=12), a slightly higher dose to skin was observed with MBRT. This is expected as electron beams have higher entrance doses than photon beams. Larger volumes of future surgical skin flaps receiving higher doses have been associated with higher risk of wound complications.[4] In this study, the near-maximum dose to skin in MBRT plans were ensured to be lower than 103% of the prescription dose. This was done by placing an upper optimization constraint on a 2 mm skin contour. It must be noted that despite the higher near-maximum skin dose in these 12 MBRT plans, they do not exceed the skin dose constraint. As higher weighting is placed on achieving lower doses to skin, the optimizer will tend to reduce the proportion of electrons versus photons in the MBRT plan. Although reducing electron usage does decrease doses to skin, it also has the effect of

increasing dose to deeper normal tissue due to the resulting increase in photons. The planner must therefore make a trade-off between skin dose and normal tissue dose. As wound healing complications due to high skin dose can still be managed, a higher concern is generally placed on limiting risks of long-term sequelae associated with elevated dose to normal tissue.

In the RTOG 0630 protocol[5] and the current study, the dose to a longitudinal strip of normal tissue is constrained such that $V_{20Gy} < 50\%$. However there is no consensus on the definition of the normal tissue strip contour, which is usually left at the discretion of the radiation oncologist. Depending on the proximity of the normal tissue contour to the CTV and its extent, there is significant variance of the V_{20Gy} metric for a same plan. To avoid this inconsistency from introducing bias in the comparison of MBRT and VMAT plans, all normal tissue strips in this study were contoured according to a consistent rule described in the *Methods* section. As such, normal tissue strips in this study are representative of a proportion of the limb and, conceptually it is precisely the volume of interest given the long-term sequelae correlate with volume of normal tissue irradiated.

In current clinical practice, dose prescriptions for STS are given as dose-to-water. As such, all doses in this study have been calculated as dose-to-water to provide a fair comparison. One can question whether the conclusions of this study would remain the same if the absorbed dose-to-medium were to be reported. This is a reasonable concern as electrons are used as part of MBRT plans. The impact of scoring dose-to-medium versus dose-to-water is estimated in the *Supplementary material*. We have found that dose conversions from dose-to-water to dose-to-medium would have a clinically equivalent effect on both MBRT and VMAT doses. The conclusions of this study would therefore remain valid if dose-to-medium had been calculated.

The present study assesses the potential dosimetric benefits of an implementation of MBRT compared to the current clinical practice. To provide a representative comparison to the dose distributions being delivered to patients, no re-optimization of VMAT plans were performed. All VMAT plans were optimized on Eclipse, using AAA for dose calculation. On the other hand, MBRT was optimized with in-house algorithms featured on *Brems*. In particular, MBRT optimization was performed robustly while VMAT optimization was PTV-based. Photon-based treatment plans are not currently using robust optimization in routine clinical practice. Nevertheless, one may question if the dosimetric sparing achieved in MBRT plans can be truly attributed to its mixed modality or if it is a result of the robust optimization. Indeed, by explicitly calculating the perturbed dose distributions, the robust optimizer can achieve a more conformal MBRT plan than required when imposing isotropic PTV margins.[25] For one representative case, the MBRT plan was re-optimized non-robustly using the PTV, but otherwise identical optimization constraints. The DVH in Figure 7 shows that a PTV-optimized MBRT plan still achieves better sparing of normal tissue than VMAT. The sharp dose fall-off with depth is characteristic of electron dose distributions and cannot be featured in megavoltage photon-based treatments. Although robust optimization can be responsible for some of the healthy tissue sparing seen in MBRT plans, the contribution from the electron beams' limited penetration depth is the primary reason for MBRT's superior healthy tissue sparing.

Due to the retrospective nature of this planning study, no direct conclusions can be made on the impact of MBRT on patient outcomes and toxicities. Due to the limited cohort size obtained from a single institution, the generalizability of the dosimetric benefits found in this study may need to be confirmed on a larger multi-institutional cohort. Although the difference in dose metrics to the relevant structures were quantified, the overall plan quality of each patient was not individually scored by clinicians and the comparison between plans of either modality was not blinded. Furthermore, in this study, MBRT plans were retrospectively re-optimized and compared to clinical VMAT plans. Plans of each modality were therefore optimized by different planners who could have spent a differing length of time. This could be a potential source of bias and constitutes a limitation of the present study. As MBRT requires no modification on current linacs to be deliverable, its clinical applicability could be immediate. However, optimization of MBRT plans remains time-consuming and resource intensive. Future work will focus on alleviating the optimization's bottleneck and on investigating the applicability of MBRT to other treatment sites.

A subset of five plans were verified to be deliverable on Varian TrueBeam linacs using *Developer Mode* as part of a separate study.[41] A priori, all other plans should also be deliverable. Total delivery time for one fraction was under 15 min, with photon apertures accounting for around half the time. As all apertures were delivered at standard SAD, no intra-fraction couch translation was required. This is in contrast to previous MBRT studies that have all reported the use of shortened SSD setups for deliveries of electron apertures.[20–26,31]

5 | CONCLUSION

The purpose of this study was to investigate the dosimetric benefits of MBRT when applied to cases of STS of the extremity. To this end, a retrospective MBRT treatment planning study was performed and the resulting plans were compared to the clinically delivered VMAT plans. MBRT plans achieved clinically equivalent target coverage and homogeneity as compared to VMAT, without the need for bolus. For all patients, MBRT plans had either significantly lower or equivalent doses to normal

tissue and bone. Being deliverable on current state-of-the-art linacs without the use of electron applicators[26,31] or shortened SSD,[41] MBRT offers significant dosimetric benefits at reduced logistical cost.

ACKNOWLEDGMENTS

The authors acknowledge support from the Fonds de recherche du Québec Nature et Technologie (FRQNT) (award number 290039) and the Canadian Institutes of Health Research Foundation Grant (FDN-143257).

CONFLICT OF INTEREST STATEMENT

The authors have no relevant conflicts of interest to disclose.

DATA AVAILABILITY STATEMENT

The data that support the findings of this study are available from the corresponding author upon reasonable request.

REFERENCES

1. Siegel RL, Miller KD, Fuchs HE, Jemal A. Cancer statistics, 2022. *CA Cancer J Clin*. 2022;72(1):7-33.
2. Surveillance Research Program, National Cancer Institute. SEER*Explorer: An interactive website for SEER cancer statistics. [Online] 2023. https://seer.cancer.gov/statistics-network/explorer/
3. Salerno KE, Alektiar KM, Baldini EH, et al. Radiation therapy for treatment of soft tissue sarcoma in adults: executive summary of an astro clinical practice guideline. *Pract Radiat Oncol*. 2021;11(5):339-351.
4. O'Sullivan B, Griffin AM, Dickie CI, et al. Phase 2 study of preoperative image-guided intensity-modulated radiation therapy to reduce wound and combined modality morbidities in lower extremity soft tissue sarcoma. *Cancer*. 2013;119(10):1878-1884.
5. Wang D, Zhang Q, Eisenberg BL, et al. Significant reduction of late toxicities in patients with extremity sarcoma treated with image-guided radiation therapy to a reduced target volume: results of radiation therapy oncology group RTOG-0630 trial. *J Clin Oncol*. 2015;33(20):2231-2238. PMID: 25667281.
6. Stinson SF, Delaney TF, Greenberg J, et al. Acute and long-term effects on limb function of combined modality limb sparing therapy for extremity soft tissue sarcoma. *Int J Radiat Oncol Biol Phys*. 1991;21(6):1493-1499.
7. Lee MC, Jiang SB, Ma CM. Monte Carlo and experimental investigations of multileaf collimated electron beams for modulated electron radiation therapy. *Med Phys*. 2000;27(12):2708-2718.
8. Ma CM, Pawlicki T, Lee MC, et al. Energy- and intensity-modulated electron beams for radiotherapy. *Phys Med Biol*. 2000;45(8):2293-2311.
9. Hogstrom KR, Boyd RA, Antolak JA, Svatos MM, Faddegon BA, Rosenman JG. Dosimetry of a prototype retractable eMLC for fixed-beam electron therapy. *Med Phys*. 2004;31(3):443-462.
10. Gauer T, Albers D, Cremers F, Harmansa R, Pellegrini R, Schmidt R. Design of a computer-controlled multileaf collimator for advanced electron radiotherapy. *Phys Med Biol*. 2006;51(23):5987-6003.
11. Gauer T, Sokoll J, Cremers F, Harmansa R, Luzzara M, Schmidt R. Characterization of an add-on multileaf collimator for electron beam therapy. *Phys Med Biol*. 2008;53(4):1071-1085.
12. Al-Yahya K, Verhaegen F, Seuntjens J. Design and dosimetry of a few leaf electron collimator for energy modulated electron therapy. *Med Phys*. 2007;34(12):4782-4791.
13. Alexander A, Deblois F, Seuntjens J. Toward automatic field selection and planning using Monte Carlo-based direct aperture optimization in modulated electron radiotherapy. *Phys Med Biol*. 2010;55(16):4563-4576.
14. Connell T, Alexander A, Papaconstadopoulos P, Serban M, Devic S, Seuntjens J. Delivery validation of an automated modulated electron radiotherapy plan. *Med Phys*. 2014;41(6):061715.
15. Du Plessis FC, Leal A, Stathakis S, Xiong W, Ma CM. Characterization of megavoltage electron beams delivered through a photon multi-leaf collimator (pMLC). *Phys Med Biol*. 2006;51(8):2113-2129.
16. Klein EE, Vicic M, Ma CM, Low DA, Drzymala RE. Validation of calculations for electrons modulated with conventional photon multileaf collimators. *Phys Med Biol*. 2008;53(5):1183-1208.
17. Salguero FJ, Palma B, Arrans R, Rosello J, Leal A. Modulated electron radiotherapy treatment planning using a photon multileaf collimator for post-mastectomized chest walls. *Radiother Oncol*. 2009;93(3):625-632.
18. Henzen D, Manser P, Frei D, et al. Beamlet based direct aperture optimization for MERT using a photon MLC. *Med Phys*. 2014;41(12):121711.
19. Alexander A, Soisson E, Renaud MA, Seuntjens J. Direct aperture optimization for FLEC-based MERT and its application in mixed beam radiotherapy. *Med Phys*. 2012;39(8):4820-4831.
20. Palma BA, Sánchez AU, Salguero FJ, et al. Combined modulated electron and photon beams planned by a Monte-Carlo-based optimization procedure for accelerated partial breast irradiation. *Phys Med Biol*. 2012;57(5):1191-1202.
21. Míguez C, Jiménez-Ortega E, Palma BA, et al. Clinical implementation of combined modulated electron and photon beams with conventional MLC for accelerated partial breast irradiation. *Radiother Oncol*. 2017;124(1):124-129.
22. Renaud MA, Serban M, Seuntjens J. On mixed electron-photon radiation therapy optimization using the column generation approach. *Med Phys*. 2017;44(8):4287-4298.
23. Mueller S, Fix MK, Joosten A, et al. Simultaneous optimization of photons and electrons for mixed beam radiotherapy. *Phys Med Biol*. 2017;62(14):5840-5860.
24. Mueller S, Manser P, Volken W, et al. Part 2: dynamic mixed beam radiotherapy (dymber): photon dynamic trajectories combined with modulated electron beams. *Med Phys*. 2018;45(9):4213-4226.
25. Renaud MA, Serban M, Seuntjens J. Robust mixed electron-photon radiation therapy optimization. *Med Phys*. 2019;46(3):1384-1396.
26. Heath E, Mueller S, Guyer G, et al. Implementation and experimental validation of a robust hybrid direct aperture optimization approach for mixed-beam radiotherapy. *Med Phys*. 2021;48(11):7299-7312.
27. Klein EE, Li Z, Low DA. Feasibility study of multileaf collimated electrons with a scattering foil based accelerator. *Radiother Oncol*. 1996;41(2):189-196.
28. Mueller S, Fix MK, Henzen D, et al. Electron beam collimation with a photon MLC for standard electron treatments. *Phys Med Biol*. 2018;63(2):025 017.
29. ICRU. Report 83: Prescribing, Recording, and Reporting Photon-Beam Intensity-Modulated Radiation Therapy (IMRT). *J ICRU*. 2010;10(1).
30. Unkelbach J, Paganetti H. Robust proton treatment planning: physical and biological optimization. *Semin Radiat Oncol*. 2018;28(2):88-96.
31. Heng VJ, Serban M, Seuntjens J, Renaud MA. Ion chamber and film-based quality assurance of mixed electron-photon radiation therapy. *Med Phys*. 2021;48(9):5382-5395.
32. Hansen CR, Crijns W, Hussein M, et al. Radiotherapy treatment plannINg study guidelines (RATING): a framework for setting up and reporting on scientific treatment planning studies. *Radiother Oncol*. 2020;153:67-78.

33. Renaud M, DeBlois F. Webtps: a complete web application for monte carlo treatment plan recalculation. *Int J Radiat Oncol Biol Phys*. 2013;87(2):S625.
34. Jabbari K, Keall P, Seuntjens J. Considerations and limitations of fast Monte Carlo electron transport in radiation therapy based on precalculated data. *Med Phys*. 2009;36(2):530.
35. Renaud MA, Roberge D, Seuntjens J. Latent uncertainties of the precalculated track Monte Carlo method. *Med Phys*. 2015;42(1):479-490.
36. Kawrakow I, Rogers DWO, Mainegra-Hing E, Tessier F, Townson RW, Walters BRB. *Egsnrc toolkit for monte carlo simulation of ionizing radiation transport*. 2000. https://doi.org/10.4224/40001303 [release v2021]
37. Holt GE, Griffin AM, Pintilie M, et al. Fractures following radiotherapy and limb-salvage surgery for lower extremity soft-tissue sarcomas: a comparison of high-dose and low-dose radiotherapy. *J Bone Joint Surg*. 2005;87(2):315-319.
38. Baldini EH, Lapidus MR, Wang Q, et al. Predictors for major wound complications following preoperative radiotherapy and surgery for soft-tissue sarcoma of the extremities and trunk: importance of tumor proximity to skin surface. *Ann Surg Oncol*. 2013;20(5):1494-1499.
39. LeBrun DG, Guttmann DM, Shabason JE, Levin WP, Kovach SJ, Weber KL. Predictors of wound complications following radiation and surgical resection of soft tissue sarcomas. *Sarcoma*. 2017;2017:5465 130.
40. Hymes SR, Strom EA, Fife C. Radiation dermatitis: clinical presentation, pathophysiology, and treatment 2006. *J Am Acad Dermatol*. 2006;54(1):28-46.
41. Tai YM, Heng VJ, Renaud MA, Serban M, Seuntjens J. Quality assurance for mixed electron-photon beam radiation therapy using treatment log files and MapCHECK. Manuscript submitted for publication.
42. Reynaert N, Crop F, Sterpin E, Kawrakow I, Palmans H. On the conversion of dose to bone to dose to water in radiotherapy treatment planning systems. *Phys Imaging Radiat Oncol*. 2018;5:26-30.
43. Berger M, Oursey J, Zucker M. ESTAR, PSTAR, and ASTAR: computer programs for calculating stopping-power and range tables for electrons, protons, and helium ions (version 1.2.3). [Online]. 2005. http://physics.nist.gov/Star
44. Berger M, Hubbell J, Seltzer S, Coursey J, Zucker D. Xcom: Photon cross section database (version 1.5). [Online]. 2010. http://physics.nist.gov/xcom

SUPPORTING INFORMATION

Additional supporting information can be found online in the Supporting Information section at the end of this article.

How to cite this article: Heng VJ, Serban M, Renaud M-A, Freeman C, Seuntjens J. Robust mixed electron-photon radiation therapy planning for soft tissue sarcoma. *Med Phys*. 2023;50:6502–6513. https://doi.org/10.1002/mp.16709